Optics Communications 297 (2013) 190–193

Contents lists available at SciVerse ScienceDirect

Optics Communications

journal homepage: www.elsevier.com/locate/optcom

All-optical EIT-like phenomenon in plasmonic stub waveguide with ring resonator

Yudong Cui *, Chao Zeng *

State Key Laboratory of Transient Optics and Photonics, Xi'an Institute of Optics and Precision Mechanics, Chinese Academy of Sciences, Xi'an 710119, China

ARTICLE INFO

Article history:
Received 19 September 2012
Received in revised form
15 January 2013
Accepted 19 January 2013
Available online 13 February 2013

Keywords:
Surface plasmons
Optical resonator
Electromagnetically induced transparency

ABSTRACT

An optical phenomenon analogous to electromagnetically induced transparency (EIT) has been proposed and investigated numerically in a plasmonic system, which is composed of a single stub-shaped metal–insulator–metal (MIM) waveguide coupled with a ring resonator. The transmission properties of the system are simulated by the finite-difference time-domain (FDTD) method. The bandwidth of the EIT-like spectrum is mainly dependent on the coupling distance between the stub and ring resonator. The red-shift of EIT-like peak is nearly linearly proportional to the increase in the radius and the refractive index of ring resonator, as is confirmed by the theoretical calculations. Our compact plasmonic structure may find potential applications in highly integrated optical circuits, such as nanoscale filters and optical switching.

1. Introduction

Surface plasmons (SPs) are essentially light waves trapped on the interface of metal and dielectric and coupled with the oscillating collectively free electrons [1]. Due to their near-field characteristics and the associated field enhancement, SPs show great potential as a new class of subwavelength photonic devices to minimize integrated optical devices and circuits [1,2]. So far, numerous SP devices have been investigated, such as wavelength demultiplexers [3–5], Bragg reflectors [6,7], plasmonic nanosensors [8], absorbers [9], filters [10–12], splitters [13], all-optical switching [14], and slow-light systems [15]. Among plasmonic structures, metal–insulator–metal (MIM) waveguides draw much attention because of the deep-subwavelength confinement of light and relatively simple fabrication [2,16]. They provide a promising platform to realize nanoscale photonic functionality and features, such as optical bistability [17–19] and electromagnetically induced transparency (EIT)-like effect [20]. EIT is a quantum mechanical effect which occurs in three-level atomic systems due to the quantum destructive interference between the excitation pathways [21–26]. EIT effect has broad applications in enhanced optical nonlinearities, optical data storage, and ultrafast switching for the strong dispersion in the transparent windows [23,25]. However, the conventional realization of EIT is unsuitable for chip-scale implementation owing to the requirements of rigorous conditions, which has catalyzed an ongoing search for mimicking EIT in classical systems [23]. A number of classical configurations such as coupled optical resonator systems have been proposed for the realization of EIT-like effect [21], which is known as coupled-resonator induced transparency (CRIT). The CRIT effect in coupled resonator systems is remarkably analogous to the conventional EIT in atomic systems [26]. In particular, the structures based on SPs are found to be another promising addition for the realization of all-optical EIT-like schemes [22]. The recent researches show that an all-optical analogous to EIT can occur in plasmonic structures with optical cavities on the basis of the destructive interference between coupled resonators [20,23–26]. For example, Lu et al. reported observations of EIT-like resonance effect in waveguide-coupled resonators [24] and a multi-nanoresonator-coupled waveguide system [25]. And Wang et al. realized a significant slow-light effect based on EIT-like phenomenon [15]. The results open up a new pathway to realize light manipulation and transmission in nanoscale devices [23].

In this paper, we investigate numerically an all-optical analog of EIT effect in a novel plasmonic system, which consists of a stub-shaped MIM waveguide coupled with a ring resonator. By the FDTD simulations, it is found that the transmission properties of the transparency effect can be manipulated by adjusting the geometrical parameters, such as the coupling distance between the stub and the ring resonator, the stub length, the radius and refractive index of ring resonator. Our results can find potential applications for nanoscale wavelength-filtering and optical switching elements in highly-integrated optical circuits.

2. Model and theory

Fig. 1 illustrates the schematic of the plasmonic structure, which is composed of a stub-shaped MIM waveguide coupled

* Corresponding authors. Tel.: 008688888033.
E-mail addresses: cuiyudong@opt.cn (Y. Cui), zengchao@opt.cn (C. Zeng).

0030-4018/$ - see front matter
http://dx.doi.org/10.1016/j.optcom.2013.01.061

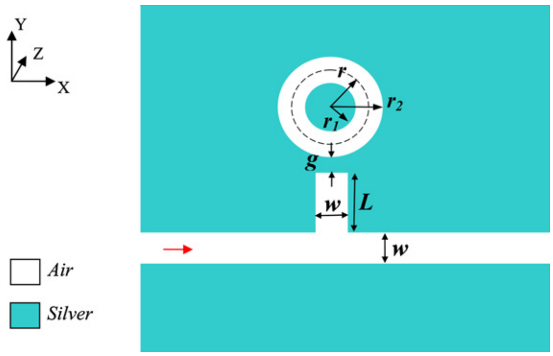

Fig. 1. Schematic of the plasmonic structure. g: Coupling length between the stub and ring resonator; w: the width of the waveguide and stub; r: the radius of the ring resonator, $r=(r_1+r_2)/2$; L: the length of the stub.

with a ring resonator. The outer and inner radii of the ring resonator are r_1 and r_2, respectively, and the radius of the ring resonator is the average of the inner and outer radii, $r=(r_1+r_2)/2$, as described by the dashed curve in Fig. 1. L is the length of the stub structure, w is the width of the waveguide and stub, and g represents the coupling distance between the stub and the ring resonator. When a TM-polarized plane light wave is coupled into the plasmonic structure, the SP waves will be excited and confined in the dielectric layer of the MIM waveguide [7]. The dielectric material in the waveguide system is set as air with refractive index of 1. The metal is assumed as silver, whose relative permittivity can be described by the Drude model [10],

$$\varepsilon_m(\omega)=\varepsilon_\infty-\frac{\omega_p^2}{\omega(\omega+i\gamma)} \tag{1}$$

where ε_∞ is the dielectric constant at infinite frequency, ω_p is the bulk plasma frequency of free conduction electrons, γ stands for the damping frequency of the electron oscillations, and ω is the angular frequency of incident light in vacuum. These parameters for silver can be set to be $\varepsilon_\infty=3.7$, $\omega_p=9.1$ eV, and $\gamma=0.018$ eV [25]. The imaginary part of the relative permittivity corresponds to the ohmic loss which influences the transmission of SPs in the plasmonic waveguide structure. To study the transmission properties, we assume that the light wave is input at the left side and outputted at the right side of the waveguide. P_i and P_t represent the power at incident and transmitted ports, respectively, and then we define the transmission efficiency as $T=P_t/P_i$ [10]. The FDTD method is employed to investigate the optical properties in our structure [27].

The ring-shaped nanocavity acts as a ring resonator. The standing wave modes which satisfy the resonant condition will be excited in the resonator according to the theory of ring resonator [28]. The characteristic equation can be given by

$$\frac{J_n'(kr_2)}{J_n'(kr_1)}-\frac{N_n'(kr_2)}{N_n'(kr_1)}=0 \tag{2}$$

where $k=\omega c(\varepsilon_r)^{1/2}$. $\varepsilon_r=n_{eff}^2$ Is the effective relative permittivity. n_{eff} Is the effective refractive index of the ring, which can be achieved by solving the dispersion formula [7]. J_n and $J_n{}'$ stand for the first kind Bessel function to the argument (kr) with the order n and its derivative. N_n and $N_n{}'$ are the second kind Bessel function to the argument (kr) with the order n and its derivative [28]. The resonant wavelengths in ring resonator can be obtained from the above transcendent equation. From Eq. (2), the resonant wavelength depends on the radius r and the effective refractive index in the ring cavity.

3. Results and discussions

We investigate numerically the transmission characteristics of this plasmonic MIM structure by the FDTD method. The geometrical parameters of the structure are set as $L=120$ nm, $r_1=115$ nm, $r_2=65$ nm, $r=90$ nm, $w=50$ nm, and $g=20$ nm. Fig. 2(a) shows the transmission spectra without and with the ring resonator. Without the ring resonator, the transmission spectrum exhibits a spectral dip at the resonance wavelength of 807 nm due to the destructive interference between the incident wave and escaped power from the resonator [25]. When the incident light is far from the resonance wavelength, the resonant and destructive interference effect is weaker in the stub and the transmission spectrum is higher. When the stub is coupled with a ring resonator, the transmission spectrum exhibits a narrow transparency peak in the transmission dip near the resonant wavelength of the ring resonator. This is a typical EIT-like spectral response, which is derived from a special coherent effect: the coherent interference between the two optical pathways, namely, the direct excitation of resonant mode in the stub by the external light and the excitation by coupling with the ring cavity [29]. The peak value of the transmission spectrum is about 70% (not unity) due to the ohmic loss in the plasmonic structure. Fig. 2(b) and (c) shows the field distributions of $|H_z|$ at the EIT-like transparency peak of 807 nm without and with a ring resonator. As shown in Fig. 2(b), the incident lights are reflected in the stub-shaped waveguide, whereas they can pass through the waveguide with the ring resonator, as can be seen in Fig. 2(c). The results are consistent with the spectral response in Fig. 2(a). It is worthy noting that the electromagnetic field in the stub is weakened due to the interference effect when the stub couples with the ring cavity. There exist strongly enhanced fields in ring cavity due to the excitation of the resonant mode.

The coupling distance g between the stub and ring resonator is an important factor influencing the transmission properties. The transmission spectra with different coupling distances are shown in Fig. 3. It is found that the induced transparency wavelength is nearly invariable owing to the fixed resonant condition of ring

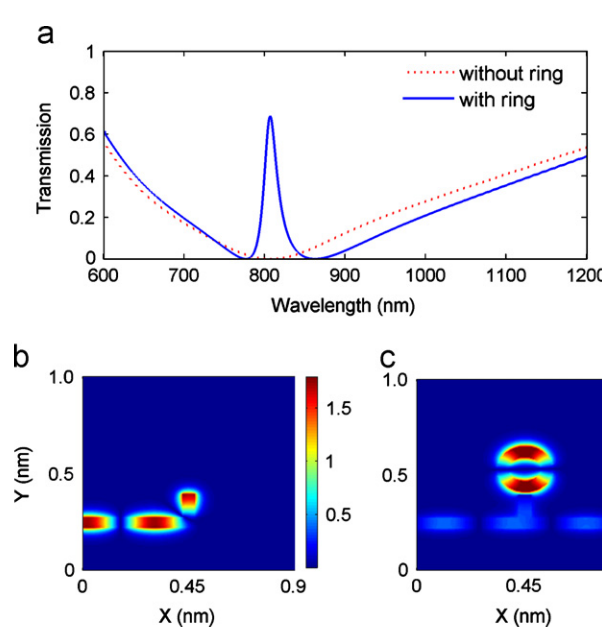

Fig. 2. (a) Transmission spectra without (dashed curve) and with (solid curve) the ring resonator. The geometrical parameters are set as $L=120$ nm, $r_1=115$ nm, $r_2=65$ nm, $r=90$ nm, $w=50$ nm, and $g=20$ nm. (b and c) Field distributions $|H_z|$ without and with the ring resonator for the incident wavelength of 807 nm (i.e., EIT-like peak wavelength).

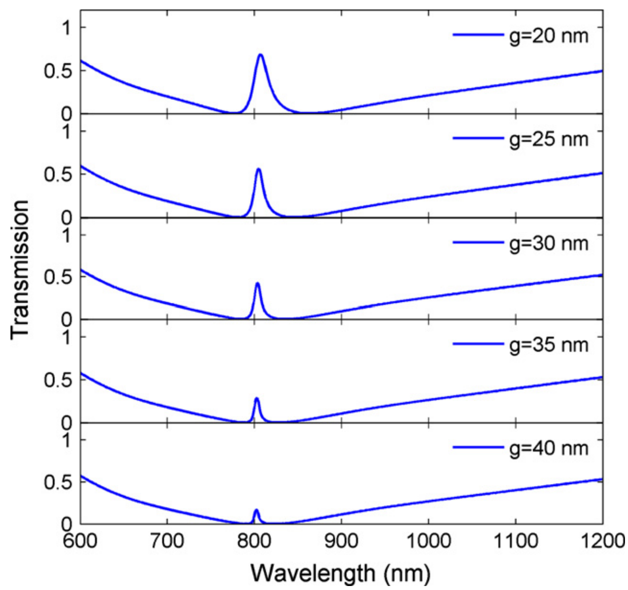

Fig. 3. Transmission spectra with different coupling distances g. The other parameters are $L=120$ nm, $r_1=115$ nm, $r_2=65$ nm, $r=90$ nm and $w=50$ nm.

resonator. While a larger coupled distance induces a narrower transmission spectral bandwidth but a reducing EIT-like peak transmission. There is a tradeoff between the peak value of transmission spectrum and the spectral bandwidth. This result offers a convenient approach to control the spectral bandwidth of the transparency resonance.

From Eq. (2), the resonant wavelength of ring resonator acts as a function of the radius r. The influences of r on the transmission spectrum are calculated theoretically and investigated by the FDTD simulation. As shown in Fig. 4(a), the transmission spectral response is sensitive to the change in the radius of ring cavity, and the EIT-like peak performs a redshift with increasing the radius. The transparency peak exhibits an approximately linear relation with the radius of ring resonator, as can be seen in Fig. 4(b). Transmission spectra with different refractive indices of the ring cavity are also investigated, as shown in Fig. 5(a). The transparency peak has a redshift with the increase of the refractive index in ring cavity, as depicted in Fig. 5(b). The EIT-like resonant peak nearly possesses a linear relation with refractive index. The theoretical results obtained by solving Eq. (2) are consistent with the FDTD simulations. According to the dispersion relations [7], the real part of effective refractive index is assumed as 1.4 for the 50 nm ring waveguide with air in calculations of Fig. 4(b). The effective refractive indices are set as 1.4, 1.468, 1.536, 1.604, 1.672, and 1.741 for the refractive indices of 1.0, 1.05, 1.10, 1.15, 1.20, and 1.25, respectively. The small imaginary part can be neglected, which corresponds to the propagation loss. However, there is a little difference between the FDTD simulations and the theoretical results, which is in agreement with the results in [28]. Firstly, the effective relative refractive index is inexactly assumed as a constant in the whole ring. Secondly, the coupling length between the ring and the stub are finite, thus the effective refractive index in the coupling zone is different from that in other position of the ring. Additionally, the curvature of the ring cavity also affects the effective refractive index. The smaller curvature will give rise to the theoretical calculation closer to the simulation results [28].

Finally, we investigate the influence of the stub length on EIT-like transmission spectral response, as shown in Fig. 6. The location of the transmission dip exhibits a redshift with the increase of L [30]. The EIT-like resonance wavelength has no

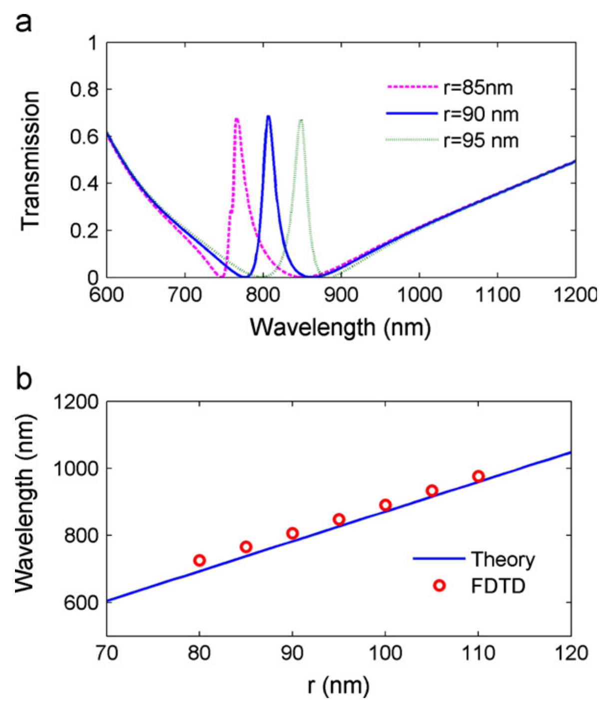

Fig. 4. (a) Transmission spectra with different radii r of the ring resonator. The other parameters are $L=120$ nm, $w=50$ nm, and $g=20$ nm. The thickness of the ring waveguide is fixed as 50 nm (i.e., $r_1-r_2=50$ nm). (b) EIT-like peak wavelength versus r, which is calculated by FDTD simulations (circles) and theoretical formula (line).

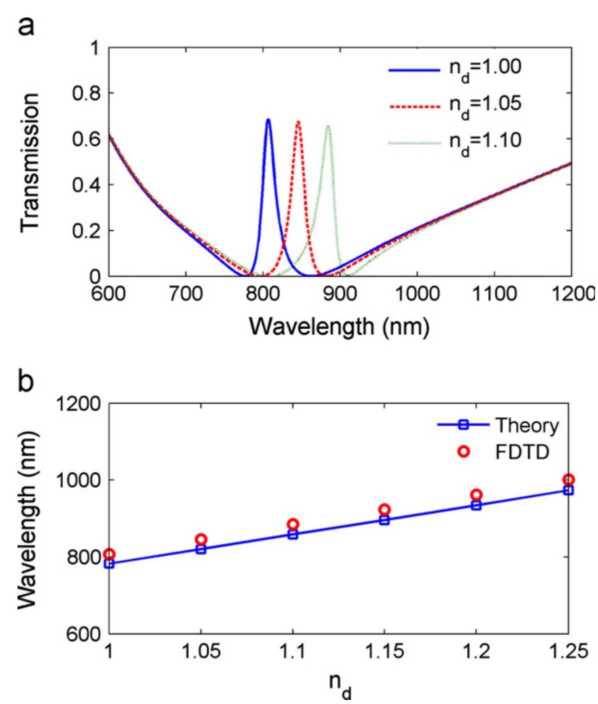

Fig. 5. (a) Transmission spectra with different refractive indices n_d of ring resonator. The geometrical parameters are $L=120$ nm, $r_1=115$ nm, $r_2=65$ nm, $r=90$ nm, $w=50$ nm, and $g=20$ nm. (b) EIT-like peak wavelength versus n_d, which is calculated by FDTD simulations (circles) and theoretical formula (line).

obvious shift as the resonant modes in the ring resonator are invariable. Additionally, the transmission spectra exhibit an asymmetric profile, which is regarded as Fano asymmetry in plasmonic waveguide platform EIT-like systems [31]. However,

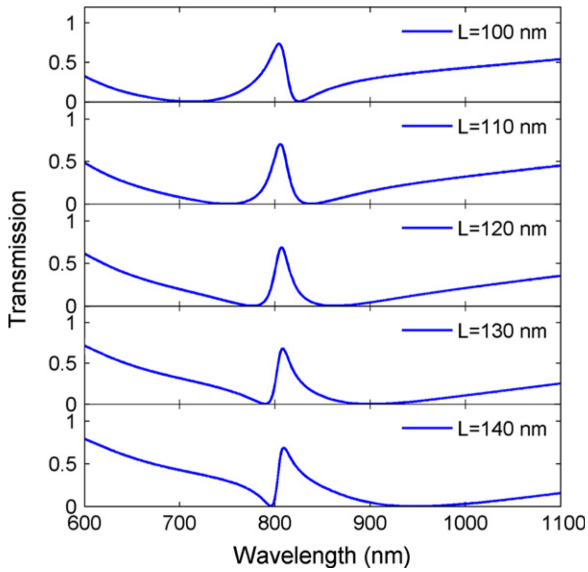

Fig. 6. EIT-like spectral response with different lengths of the stub. The geometrical parameters are $r_1=115$ nm, $r_2=65$ nm, $r=90$ nm, $w=50$ nm and $g=20$ nm.

the transmission spectral line shape exhibits an obvious change with altering the resonance wavelength of the stub, which is controlled by adjusting the length of the stub.

4. Conclusions

In this paper, the stub-shaped MIM plasmonic waveguide coupled with a ring resonator has been proposed and investigated numerically. An all-optical analog of EIT effect is observed in this novel plasmonic structure, which is simulated by the FDTD method. By adjusting the coupling distance between the stub and the ring cavity, the bandwidth of the transmission spectrum can be controlled artificially. The shape of the transmission spectrum is influenced by the length of the stub. The numerical solutions of characteristic equation show that the transmission peak wavelength exhibits a nearly linear redshift with the change in the radius and refractive index of the ring, which are identical with the FDTD results. These results provide a possibility for the realization of tunable nanoplasmonic filtering and switching devices, which can find excellent applications in highly integrated optical circuits and signal processing.

Acknowledgments

This work was supported by the National Natural Science Foundation of China under Grants 10874239, 10604066, and 11204368.

References

[1] W.L. Barnes, A. Dereux, T.W. Ebbesen, Nature 424 (2003) 824.
[2] R. Zia, J.A. Schuller, M.L. Brongersma, Materials Today 9 (2006) 20.
[3] H. Lu, X. Liu, L. Wang, D. Mao, Y. Gong, Applied Physics B 103 (2011) 877; H. Lu, X. Liu, L. Wang, D. Mao, Y. Gong, Optics Express 19 (2011) 12885; H. Lu, X. Liu, Y. Gong, D. Mao, G. Wang, Journal of the Optical Society of America B 28 (2011) 1616.
[4] G. Wang, H. Lu, X. Liu, D. Mao, L. Duan, Optics Express 19 (2011) 3513.
[5] F. Hu, H. Yi, Z. Zhou, Optics Letters 36 (2011) 1500.
[6] Y. Gong, L. Wang, X. Hu, X. Li, X. Liu, Optics Express 17 (2009) 13727.
[7] J. Park, H. Kim, B. Lee, Optics Express 16 (2008) 413.
[8] H. Lu, X. Liu, D. Mao, G. Wang, Optics Letters 37 (2012) 3780; D.V. Oosten, M. Spasenovic, L. Kuipers, Nano Letters 10 (2010) 286.
[9] Y. Gong, Z. Li, J. Fu, Y. Chen, G. Wang, H. Lu, L. Wang, X. Liu, Optics Express 19 (2011) 10193; Y. Gong, X. Liu, L. Wang, H. Lu, G. Wang, Optics Express 19 (2011) 9759; Y. Gong, X. Liu, L. Wang, H. Lu, G. Wang, Optics Express 19 (2011) 18393.
[10] H. Lu, X.M. Liu, D. Mao, L. Wang, Y. Gong, Optics Express 18 (2010) 17922.
[11] Y. Gong, X. Liu, L. Wang, Optics Letters 35 (2010) 285.
[12] H. Lu, X. Liu, Y. Gong, L. Wang, D. Mao, Optics Communication 284 (2011) 2613.
[13] G. Veronis, S. Fan, Applied Physics Letters 87 (2005) 131102.
[14] H. Lu, X. Liu, L. Wang, Y. Gong, D. Mao, Optics Express 19 (2011) 2910; G. Wang, H. Lu, X. Liu, Y. Gong, Nanotechnology 23 (2012) 444009.
[15] G. Wang, H. Lu, X. Liu, Applied Physics Letters 101 (2012) 013111; G. Wang, H. Lu, X. Liu, Optics Express 20 (2012) 20902; G. Wang, H. Lu, X. Liu, Optics Letters 38 (2013) 558.
[16] J.A. Dionne, L.A. Sweatlock, H.A. Atwater, Physical Review B 73 (2006) 035407.
[17] G. Wang, H. Lu, X. Liu, Y. Gong, L. Wang, Applied Optics 50 (2011) 5287.
[18] Y. Shen, G. Wang, Optics Express 16 (2008) 8421.
[19] H. Lu, X. Liu, Y. Gong, D. Mao, L. Wang, Applied Optics 50 (2011) 1307.
[20] Z. Han, S.I. Bozhevolnyi, Optics Express 19 (2011) 3251.
[21] D.D. Smith, H. Chang, K.A. Fuller, A.T. Rosenberger, R.W. Boyd, Physical Review A 69 (2004) 063804.
[22] S. Zhang, D. Genov, Y. Wang, M. Liu, X. Zhang, Physical Review Letters 101 (2008) 047401.
[23] R.D. Kekatpure, E.S. Barnard, W. Cai, M.L. Brongersma, Physical Review Letters 104 (2010) 243902.
[24] H. Lu, X. Liu, D. Mao, Y. Gong, G. Wang, Optics Letters 36 (2011) 3233.
[25] H. Lu, X. Liu, D. Mao, Physical Review A 85 (2012) 053803.
[26] Y. Xiao, X. Zou, W. Jiang, Y. Chen, G. Guo, Physical Review A 75 (2007) 063833.
[27] A. Taflove, S.C. Hagness, Computational Electro-dynamics: The Finite-Difference Time-Domain Method, 2nd ed., Norwood, MA: Artech House, 2000.
[28] T. Wang, X. Wen, C. Yin, H. Wang, Optics Express 17 (2009) 24096.
[29] H. Lu, X. Liu, G. Wang, D. Mao, Nanotechnology 23 (2012) 444003.
[30] Y. Gong, X. Liu, L. Wang, Y. Zhang, Optics Communications 284 (2011) 795.
[31] X. Piao, S. Yu, N. Park, Optics Express 20 (2012) 18994.